RESEARCH ARTICLE

SCR7, an inhibitor of NHEJ can sensitize tumor cells to ionization radiation

Vidya Gopalakrishnan[1,2,3] | Shivangi Sharma[1,2] | Ujjayinee Ray[1] |
Meghana Manjunath[2,4] | Divya Lakshmanan[1] | Supriya V. Vartak[1] |
Vindya K. Gopinatha[1] | Mrinal Srivastava[1,5] | Mantelingu Kempegowda[6] |
Bibha Choudhary[2] ⑩ | Sathees C. Raghavan[1] ⑩

[1]Department of Biochemistry, Indian Institute of Science, Bangalore, Karnataka, India

[2]Institute of Bioinformatics and Applied Biotechnology, Electronics City, Bangalore, Karnataka, India

[3]Department of Zoology, St. Joseph's College (Autonomous), Irinjalakuda, Kerala, India

[4]Manipal Academy of Higher Education, Manipal, Karnataka, India

[5]Tata Institute of Fundamental Research, Hyderabad, Telangana, India

[6]Department of Studies in Chemistry, University of Mysore, Mysuru, Karnataka, India

Correspondence
Bibha Choudhary, Institute of Bioinformatics and Applied Biotechnology, Electronics City, Bangalore, Karnataka 560100, India.
Email: vibha@ibab.ac.in

Sathees C. Raghavan, Department of Biochemistry, Indian Institute of Science, Bangalore, Karnataka 560012, India.
Email: sathees@iisc.ac.in

Funding information
Indo-French Centre for the Promotion of Advanced Research, Grant/Award Number: IFC/5203-4/2015/131; Department of Biotechnology, Ministry of Science and Technology, Grant/Award Numbers: BT/PR23078/MED/29/1253/2017, BT/PR27952-INF/22/212/2018; Centre for the Promotion of Advanced Research, Grant/Award Number: IFC/5203-4/2015/131; DBT, Grant/Award Number: BT/PR23078/MED/29/1253/2017; IISc-DBT partnership programme, Grant/Award Number: BT/PR27952-INF/22/212/2018; Senior Research Fellowship from CSIR, India; Junior Research Fellowship (DBT, India); DST-INSPIRE Fellowship (India); Research Associateship (IISc, India)

Abstract

Nonhomologous end joining (NHEJ), one of the major DNA double-strand break repair pathways, plays a significant role in cancer cell proliferation and resistance to radio and chemotherapeutic agents. Previously, we had described a small molecule inhibitor, SCR7, which inhibited NHEJ in a DNA Ligase IV dependent manner. Here, we report that SCR7 potentiates the effect of γ-radiation (IR) that induces DNA breaks as intermediates to eradicate cancer cells. Dose fractionation studies revealed that coadministration of SCR7 and IR (0.5 Gy) in mice Dalton's lymphoma (DLA) model led to a significant reduction in mice tumor cell proliferation, which was equivalent to that observed for 2 Gy dose when both solid and liquid tumor models were used. Besides, co-treatment with SCR7 and 1 Gy of IR further improved the efficacy. Notably, there was no significant change in blood parameters, kidney and liver functions upon combinatorial treatment of SCR7 and IR. Further, the co-treatment of SCR7 and IR resulted in a significant increase in unrepaired DSBs within cancer cells compared to either of the agent alone. Anatomy, histology, and other studies in tumor models confirmed the cumulative effects of both agents in activating apoptotic pathways to induce cytotoxicity by modulating DNA damage response and repair pathways. Thus, we report that SCR7 has the potential to reduce the side effects of radiotherapy by lowering its effective dose ex vivo and in mice tumor models, with implications in cancer therapy.

Shivangi Sharma, Ujjayinee Ray, and Meghana Manjunath contributed equally to this study.

1 | INTRODUCTION

DNA double-strand breaks (DSBs) are among the most lethal types of DNA damage occurring in a cell. DSBs can occur as intermediates of the recombination process or due to metabolic stress and exposure to ionizing radiation (IR) or radiomimetic compounds.[1–6] When left unrepaired, DSBs can lead to chromosomal rearrangements resulting in oncogenesis or cell death.[7–11] Organisms have evolved with several DNA repair pathways such as homologous recombination, nonhomologous end joining (NHEJ), microhomology-mediated end joining for the repair of DSBs. In higher eukaryotes, most DSBs generated in a cell are repaired through the NHEJ pathway.[12–18]

During NHEJ, KU70/KU80 heterodimer recognizes and binds to the broken DNA ends and recruit proteins such as DNA-PKcs, Artemis, and Pol μ or λ to the repair site, resulting in end-processing of the damaged DNA. Sealing of the DNA ends is carried out by the Ligase IV–XRCC4–XLF complex, which is retained on the DNA with the help of KU heterodimer along with APLF.[14–16,19-22] The other accessory proteins, such as APLF and PAXX, are also believed to help assemble core NHEJ proteins onto the broken DNA ends.[6,21]

Radiotherapy is one of the most common and effective regimes used for cancer treatment, including breast cancer. Various reports suggest that surgery, along with radiation, can significantly reduce the recurrence rate and mortality in breast cancer.[13,23] However, studies also indicate that IR alone may not be sufficient to treat breast cancer.[24]

In classical Hodgkin's lymphoma and non-Hodgkin's lymphoma (NHL), radiotherapy is often followed by chemotherapy.[25] Although combination chemotherapy and immuno-chemotherapy have been shown to play a significant role in treating NHLs, radiation therapy continues to play an essential role against advanced stage NHL.[26,27] Studies suggest that consolidated radiation therapy has a much better effect than R-CHOP (chemotherapy with rituximab or Rituxan, and cyclophosphamide, doxorubicin, vincristine, and prednisone) alone treatment in stage III-IV DLBCL patients.[26] High levels of DSB repair in DLBCL contribute to radioresistance in cancer cells,[18,28] which could be counteracted by administering small molecules. Based on these, it appears that radiosensitizers play a vital role in lowering the radiation dose to which the lymphoma patients are exposed and can help in reducing the side effects caused by radiation.

Although radiotherapy has successfully eradicated cancer cells, the dose employed often affects normal healthy cells, leading to multiple side effects.[29] Irradiation of cells leads to DSBs, as intermediates, which activate cell death pathways.[30–33] Accumulating evidence suggests that deregulation of NHEJ proteins in cancer cells confers resistance against γ-radiation and chemotherapeutic agents.[18,24] Moreover, increased expression of NHEJ proteins like KU70/KU80 and DNA-PKcs have been reported in various cancers and some of these were correlated with radioresistance.[28,34–37] Our recent analysis of patient data using the UALCAN database has revealed elevated levels of *PRKDC* (coding for DNA-PKcs) in cholangiocarcinoma, sarcoma, cervical and esophageal carcinoma, and up to a 2-fold increase in *LIGASE4* (coding for DNA Ligase IV) in esophageal, head and neck cancer and skin cancers, compared to normal samples.[18] Polymorphisms in *LIGASE4* and *XRCC4* genes were reported in breast cancers, whereas patients bearing Ligase IV mutations or lower expression levels exhibited heightened radiosensitivity.[38,39] Thus, the inhibition or downregulation of NHEJ in cancer cells could be an effective strategy for sensitizing cancer cells to radiation and specific chemotherapeutic agents.

In a previous study, we reported the design and characterization of SCR7, a novel small molecule inhibitor of DNA Ligase IV.[40] SCR7 blocked NHEJ in a DNA Ligase IV dependent manner and inhibited tumor progression in multiple mouse models, leading to an increased life span.[40] Studies also indicated that SCR7 showed promising potential to improve radio and chemotherapy.[28,40] We also observed that parental SCR7 could get autocyclized to a stable form, which upon oxidation can result in SCR7-pyrazine.[41] Further, water-soluble versions of SCR7 and pyrazine exhibited anticancer efficacy in cell lines and tumor models.[42–44] Our data revealed that both the forms of SCR7 could block NHEJ in a Ligase IV dependent manner, although the cyclized version is Ligase IV specific inside the cells.[6,41–45]

In the present study, we find that combinatorial treatment with SCR7 and radiation led to a ≥ 2-fold reduction in the effective IR dose in multiple mouse tumor models and cancer cell lines. Coadministration of SCR7 and radiation resulted in the accumulation of unrepaired DSBs in cancer cells, activation of apoptosis, ultimately leading to cell death. Thus, SCR7 has the potential to be used in tandem with radiotherapy to reduce side effects by lowering the effective dose of radiation.

2 | MATERIALS AND METHODS

2.1 | Chemicals, reagents, and cell culture

Refer to Supporting Information for details.

2.2 | Synthesis of SCR7

Cyclized version of SCR7 possessing the same molecular formula and weight of parental SCR7 was prepared as described before[40,41] and referred henceforth as SCR7. Refer to Supporting Information for details.

2.3 | Irradiation

Samples were irradiated using Cobalt-60 gamma irradiator (BI 2000, BRIT, India) as described before.[46] Refer to Supporting Information for details.

2.4 | Evaluation of cytotoxicity in combination with radiation

To investigate the effect of SCR7 in combination with IR on cytotoxicity of cancer cells, trypan blue exclusion and MTT assays were performed, as described earlier.[47–50] Refer to Supporting Information for details.

2.5 | Cell cycle analysis

Cell cycle analysis was performed in Nalm6 cells, as described earlier.[48,51,52] Refer to Supporting Information for details.

2.6 | Immunocytochemistry

Nalm6 cells (0.25×10^5) were cultured in six-well plates for 24 h, followed by treatment with SCR7 (100 μM) alone or in conjunction with 0.25 Gy radiation. Dimethyl sulfoxide (DMSO)-treated cells served as control. After 24 h treatment, cells were harvested and processed for immunocytochemistry.[50,53,54] Refer to Supporting Information for details.

2.7 | Neutral comet assay

Following treatment with SCR7 (100 μM) alone or in conjunction with 0.25 Gy IR, Nalm6 cells (0.25×10^5) were cultured in six-well plates for 24 h and processed for comet assay as described.[55–57] Refer to Supporting Information for details.

2.8 | In vivo experiments

2.8.1 | Ethics statement

Mice were maintained as per the principles and guidelines of the ethical committee for animal care of the Indian Institute of Science following Indian National Law on animal care and use.

The experimental design of the present study was approved by the Institutional Animal Ethics Committee (CAF/Ethics/461/2015), Indian Institute of Science, Bangalore, India.

2.9 | Animals

Swiss albino mice 6–8 weeks old, weighing 18–22 g were obtained and were maintained as per the guidelines of the animal ethics committee following Indian National Law on animal care and use in the animal house, central animal facility, Indian Institute of Science (IISc), Bangalore, India. Refer to Supporting Information for details.

2.10 | Induction of solid and liquid tumor with Dalton's lymphoma ascites (DLA) cells

DLA tumor cells were used to develop both solid and liquid tumors in mice, as described previously.[40,58,59] Refer to Supporting Information for details.

2.11 | Evaluation of the combinatorial effect of SCR7 and γ-irradiation on tumor mouse models

To evaluate the antiproliferative effects of SCR7 in conjunction with radiation on tumor progression, mouse DLA tumor models (solid and liquid) were used. The tumor progression was determined by measuring the diameters of developing tumor using vernier calipers once in 4 days and total tumor volume was calculated using the formula $V = 0.5ab^2$, where a and b indicate the major and minor diameter, respectively.[58,60–62] At the end of 20th day of the treatment, a representative animal from each group was sacrificed by cervical dislocation and tissues were collected and stored for future experiments. Experiments were repeated for a minimum of two independent times. Refer to Supporting Information for details on DLA solid and liquid tumor models.

To check the longevity of the treated animals, the mice bearing DLA tumors were maintained for a maximum of 45 days posttreatment and then sacrificed. Mice treated with 0.5 Gy radiation, SCR7 (10 mg/kg), or coadministered with both were used for the study ($n = 5$, per group). The percentage of survival was calculated and compared with that of control animals. The survival pattern of treated animals was recorded to that of tumor control, and % increase in lifespan was calculated using the formula $[(T − C)/C]^*100$, where T indicates the number of days the treated animals survived up to their sacrifice period and C indicates the number of days tumor animals survived.[40,53,58,60–62]

2.12 | Histopathological evaluation

Thigh and liver tissues were collected from normal (no tumor), untreated mice with tumor, and tumor-bearing mice posttreatment (SCR7 in

conjunction with radiation) and processed for histological sectioning as per standard protocols.[60,63] Refer to Supporting Information for details.

2.13 | Western blot analysis

DLA-induced mouse tumor samples treated with SCR7 in conjunction with radiation were used for preparing cell extracts for western blot analysis.[64–66] Refer to Supporting Information for details.

2.14 | Linear quadratic model

Reduction in tumor volume following exposure to a particular dose (D) of radiation often follows the Linear-Quadratic Model.[67–69] In the present study, Linear Quadratic Model was plotted in GraphPad Prism ver7 using the equation $Y = \exp(-1 \cdot [a \cdot X + b \cdot X^2])$, where Y is the "fraction survival" and X is the "dose."

2.15 | Combination index (CI)

The CI was calculated by analyzing data using CompuSyn software for automated computer simulation.[70] Refer to Supporting Information for details.

2.16 | Evaluation of toxic effects of SCR7 and irradiation on mice

A total of 3 animals were used per group (SCR7 alone, IR alone [0.5, 1, and 2 Gy], SCR7 + IR [0.5 Gy+SCR7, 1 Gy+SCR7, and 2 Gy+SCR7] given as three fractions). SCR7 was injected intraperitoneally (10 mg/kg; six doses every alternate day). Three animals served as control. Mice were sacrificed by cervical dislocation and blood analysis was performed as described before.[53,71] Refer to Supporting Information for details.

2.17 | Statistical analysis

The results are expressed with a standard error of the mean. All analyses were done with GraphPad software using one-way analysis of variance or Student's t test. Statistical significance was considered as, ns: not significant, $^*p < .05$, $^{**}p < .005$, $^{***}p < .0001$.

3 | RESULTS

3.1 | SCR7 potentiated the effect of IR in cancer cells

Effect of the combinatorial potential of SCR7 (25, 50, and 100 μM) along with radiation (0.25, 0.5, and 1 Gy) was evaluated in Nalm6 cells, and the percentage of viable cells was plotted (Figure 1A). Results showed that coadministration of SCR7 resulted in a significant reduction in viable cells with all doses of radiation. While SCR7 (25 μM) with 0.25 Gy radiation resulted in >50% cell death, higher concentrations (50 and 100 μM) of SCR7 with radiation (0.25 Gy) did not yield any viable cells (Figures 1A,B and S1). The combination index and isobologram were analyzed using CompuSyn software.[70] CI obtained from the software was <0.48 for SCR7 (25 μM) in combination with IR (0.25 Gy), while at higher doses, values were <0.007, suggesting a synergistic effect (Figures 1A,B and S1).
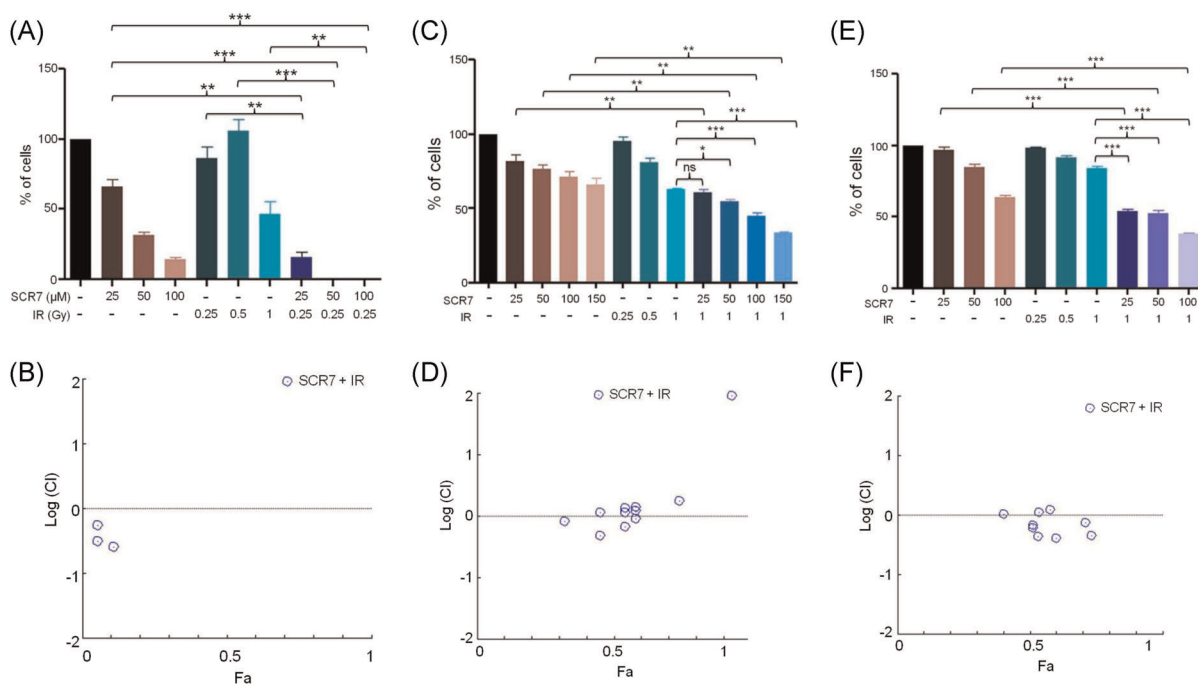
The effect of SCR7 (25, 50, and 100 μM) in combination with IR (0.25, 0.5, and 1 Gy) was further evaluated in two other leukemic cell lines, CEM and Molt4 (Figure 1C–F). It is important to note here that IC$_{50}$ of SCR7 in both CEM and Molt4 are >200 μM and 150 μM, respectively (Figure 1C,E).[40] Treatment with radiation alone did not lead to any significant cell death in these cell lines, even at 1 Gy dose (Figure 1C,E). SCR7 (100 μM) in combination with 0.25 and 0.5 Gy did not lead to much cell death in CEM and Molt4, unlike in the case of Nalm6. Interestingly, when SCR7 (50, 100 and 150 μM) was administered in CEM in conjunction with 1 Gy IR, increased cell death was observed in a dose dependent manner (Figure 1C). A combination of SCR7 (50 and 100 μM) with 1 Gy IR in Molt4 revealed >50% cell death, as compared to either of the agents alone (Figure 1E). In both cell lines, SCR7 with 1 Gy IR showed prominent cytotoxicity, with CI < 1 suggesting synergism (Figure 1D,F).

3.2 | Cell cycle analysis reveals G2/M arrest following combinatorial treatment of IR and SCR7

Cell cycle analysis was performed to examine the effect of SCR7 and γ-radiation on cell cycle progression following combinatorial treatment. Nalm6 cells were subjected to flow cytometric analysis following treatment with SCR7 (50 and 100 μM) and radiation (0.25 Gy) for 6, 12 and 24 h either alone or in combination (Figure 2A,B). Results showed a G2/M arrest following 6 and 12 h of irradiation, which did not further increase in conjunction with SCR7, although an increase in SubG1 population was evident (Figure 2A,B). The arrest was reverted at 24 h time point, probably following the repair of cellular DNA. However, there was no cell cycle arrest upon SCR7 treatment alone (Figure 2A,B). Thus, it is likely that the radiation itself primarily contributed towards cell cycle arrest observed following combined treatment.

3.3 | Combinatorial treatment of SCR7 and IR leads to the accumulation of DSBs within the cells

Since SCR7 is an inhibitor of NHEJ, we were interested in examining whether it can elevate the level of DSBs induced by γ-radiation by abrogating DSB repair. The extent of DNA damage was assessed in individual cells by performing a neutral comet assay. Results showed

FIGURE 1 Effect of SCR7, when treated in combination with radiation on viability of cancer cells. (A) Effect of SCR7 (25, 50 and 100 μM) alone and in combination with 0.25 Gy radiation in Nalm6 was plotted based on the percentage of viable cells post treatment. Cells were also treated with 0.5 and 1 Gy radiation for comparison. Error bars denote mean ± SEM (ns, not significant, *p < .05, **p < .005, ***p < .001). (B) Logarithmic combination index plot for determination of impact of SCR7 in combination with radiation in Nalm6 cells. (C) Effect of SCR7 (25, 50, 100 and 150 μM) alone and in combination with 1 Gy radiation in CEM was plotted based on the percentage of viable cells post treatment. Cells were also treated with 0.25 and 0.5 Gy radiation for comparison. (D) Logarithmic combination index plot for determination of impact of SCR7 in combination with radiation in CEM cells. (E) Effect of SCR7 (25, 50 and 100 μM) alone and in combination with 1 Gy radiation in Molt4 was plotted based on the percentage of viable cells post treatment. Cells were also treated with 0.25 and 0.5 Gy radiation for comparison. (F) Logarithmic combination index plot for determination of impact of SCR7 in combination with radiation in Molt4 cells

that Nalm6 cells treated with SCR7 in conjunction with radiation exhibited extensive DNA damage compared to independent treatment with SCR7 or irradiation (Figures 2C and 3C). The observed increase in tail moment demonstrated an elevated DNA damage in combination treated samples (Figures 2C and 3C). Thus, the above data suggest that SCR7 can potentiate radiation-induced DNA damage by several folds by blocking residual DNA repair.

As phosphorylation of histone H2AX at serine 139 position is a dominant response to DSB, resulting in the formation of γ-H2AX foci, immunofluorescence was performed after co-treatment with SCR7 (100 μM) and IR (0.25 Gy) (Figures 3A,B and S2). Nalm6 cells upon co-treatment with SCR7 and IR showed a remarkable increase in the number of γ-H2AX foci than that induced by SCR7 or irradiation alone, demonstrating the potential of SCR7 in accumulating DNA damage generated by radiation (Figures 3A,B and S2), which was consistent with our previous study.[40,41]

The combination potential of SCR7 and IR was further evaluated in HeLa cells using another DNA DSB marker, 53BP1 specific to NHEJ. HeLa cells were treated with SCR7 (100 μM) and IR (1 Gy), with different recovery periods (1, 2, 6, 12 and 24 h) (Figure 3D). Interestingly, a peak in the number of 53BP1 foci was observed at 2 h post treatment, which slowly decreased over time, and leveled at 24 h similar to that seen at 1 h. SCR7 alone showed an increase in the

number of foci at a later time point (>12 h). Although IR-induced breaks were seen as early as 1 h, the number of foci significantly reduced after 6 h, and leveled at 12 and 24 h. This suggests that although the breaks induced by IR alone were majorly repaired by 24 h, those induced by a combination of SCR7 and IR remained inside the cells, culminating in cell death (Figures 3D,E and S3).

3.4 | SCR7 significantly lowered the effective dose of radiation in the mouse DLA solid tumor model

Previously, we have observed that SCR7 inhibited tumor growth in multiple mouse tumor models, and as a preliminary investigation, we had noted that SCR7 could potentiate the effect of chemo and radiotherapy.[40] Recently, we showed that parental SCR7 and its stable autocyclized form are structural isomers, and they possess identical chemical formulas ($C18H14N4OS$), molecular weight, exact mass, and the same number of protons.[41] In the present study, we used a DLA mouse solid tumor model, to investigate the effect of SCR7 in combination with increasing IR doses.

SCR7 was administered on 12th day of tumor development. While six doses of SCR7 (10 mg/kg) were administered every alternate day, two doses of γ-radiation (0.5 or 1 Gy) were administered on
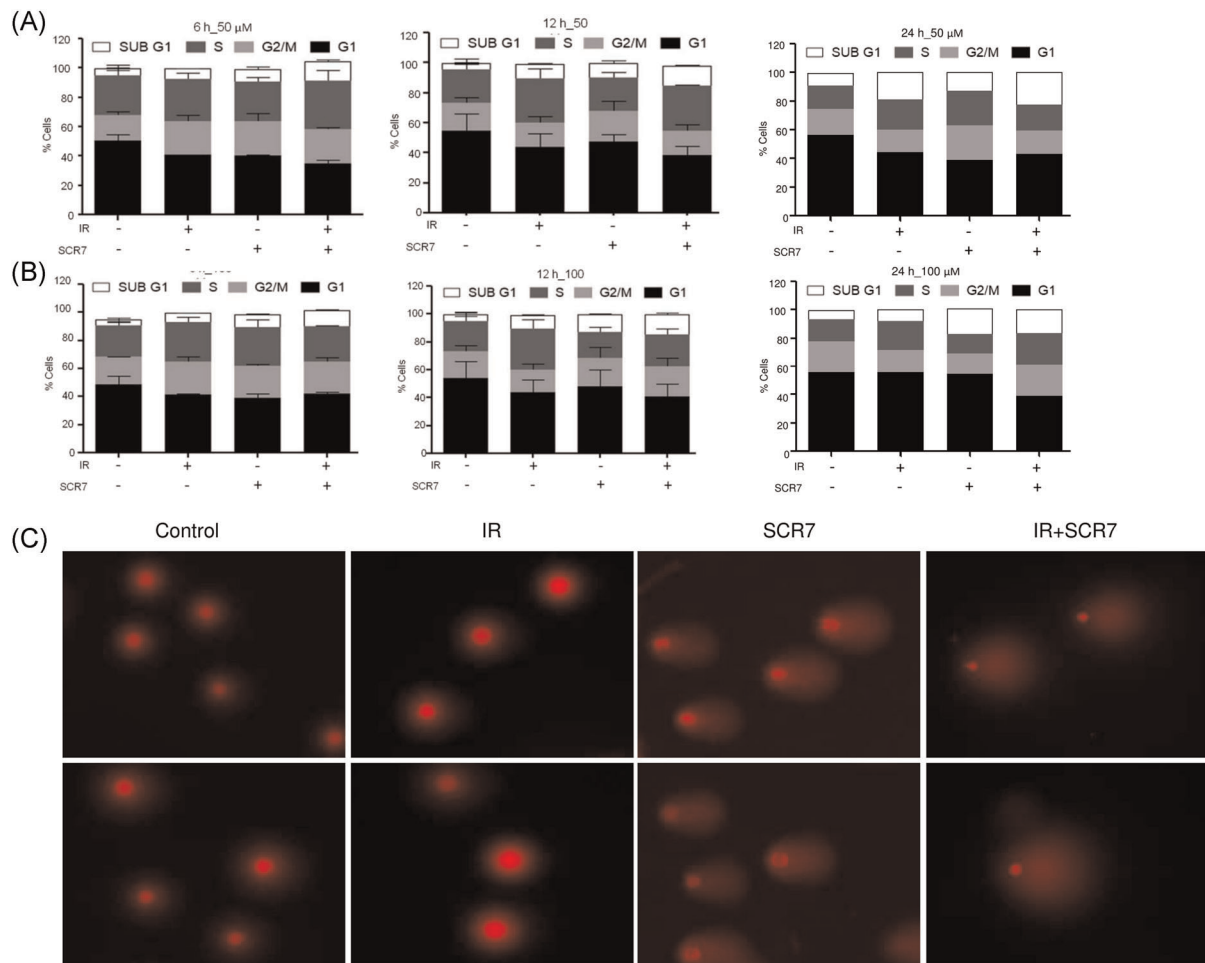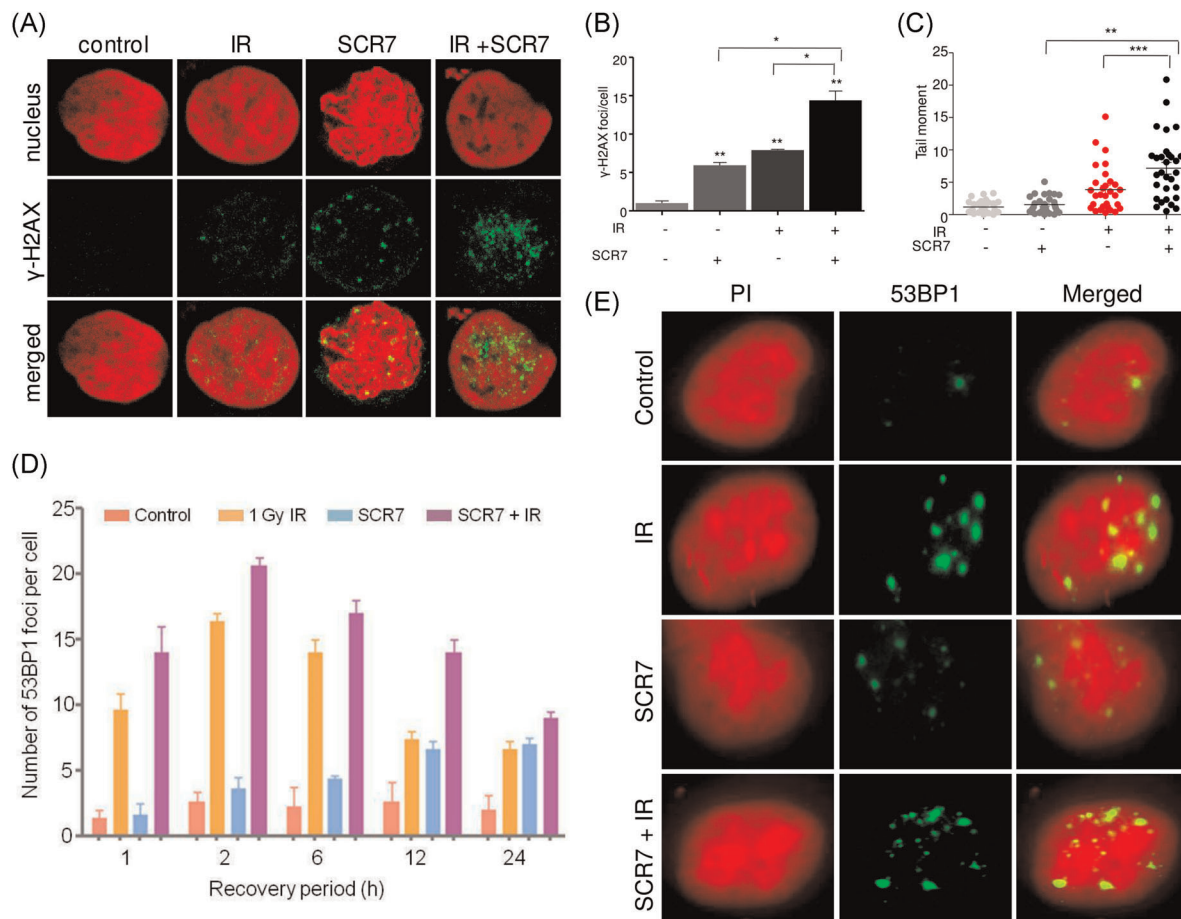
FIGURE 2 Evaluation of generation of DNA double-strand breaks (DSBs) within cells and assessment of cell cycle progression following coadministration of IR and SCR7. (A, B) Bar graph depicting cell cycle analysis following treatment with 50 μM (A) and 100 μM (B) SCR7 alone or in combination with IR (0.25 Gy) after 6, 12 and 24 h of treatment in Nalm6 cells. Error bar indicates standard deviation based on four independent experiments. (C) Representative images depicting comet assay in Nalm6 cells treated with 0.25 Gy in conjunction with SCR7 (100 μM) for a period of 24 h. Cells were electrophoresed for 25 min at 12 V followed by staining with propidium iodide (red). Each experiment was repeated a minimum of three times

1st and 3rd day of SCR7 treatment (12th and 16th day of injection of tumor cells) (Figure 4A). We observed a significant reduction in tumor volume in the combination treatment compared to either SCR7 or irradiation alone (Figure 4B–D). Importantly, we observed that SCR7 significantly potentiated tumor regression in combination cases compared to individual treatment with 0.5 and 1 Gy of IR (Figure 4B–D). Interestingly, the combination treatment of 0.5 Gy of IR and SCR7 resulted in >2-fold improvement in radiation sensitivity compared to 0.5 Gy alone (Figure 4B), which was equivalent to a dose of 1 Gy (Figure 4B,E). When SCR7 was combined with 1 Gy of IR, it improved the efficacy of radiation by >2-fold, equivalent to or even higher than 2 Gy irradiation alone (Figure 4C). The impact was even more pronounced when tumor regression was analyzed on 24th day (Figure 4E,F). Further, plotting of tumor volume against days of tumor development for DLA as a nonlinear quadratic graph revealed that treatment of 0.5 Gy combined with SCR7 exhibited an effect equivalent to that of 2 Gy alone (Figure 4G).

3.5 | SCR7 potentiated the effect of radiation in the DLA mouse liquid tumor model and improved the survivability of animals

A significant reduction in tumor volume was observed upon coadministration of SCR7 with 0.5 or 1 Gy of radiation, compared to that of IR alone, when the DLA liquid tumor model was used for the study (Figure 5A–C). Interestingly, a combination of 0.5 Gy IR and SCR7 resulted in tumor regression, with >2-fold more radiation sensitivity than 2 Gy radiation (Figure 5A). Besides, co-treatment of SCR7 with 1 Gy IR led to >2-fold improvement in radiation sensitivity compared to same dose of radiation alone (Figure 5B,C).

We examined the effect of combined treatment on the survival of mice until 45 days following coadministration of 0.5 Gy IR and SCR7 in the DLA tumor model. Results showed that while all untreated mice died due to tumor by 42nd day (control), all the mice that underwent combination treatment survived till the entire

FIGURE 3 Evaluation of generation of DNA double-strand breaks (DSBs) within cells using DNA damage markers following coadministration of IR and SCR7. (A) Representative images depicting γ-H2AX foci formation in Nalm6 cells treated with 0.25 Gy IR, along with SCR7 (100 μM) for a period of 24 h. Control cells were sham irradiated and dimethyl sulfoxide (DMSO)-treated cells served as vehicle control. γ-H2AX is immunostained using fluorescein isothiocyanate (FITC) (green), whereas the nucleus is counterstained with propidium iodide (red). Each experiment was repeated a minimum of three independent times. (B) Bar graph showing an average number of γ-H2AX foci per cell. A minimum of 100 cells were analyzed per group and foci per cell were plotted as a bar graph showing mean ± *SEM* (ns: not significant, *$p < .05$, **$p < .005$, ***$p < .0001$). (C) Scatter plot showing tail moment of Nalm6 cells as calculated and analyzed by CometScore software depicting mean ± *SEM* (ns: not significant, *$p < .05$, **$p < .005$, ***$p < .0001$). (D) Bar graphs depicting number of 53BP1 foci in HeLa cells post treatment with SCR7 (100 μM) and radiation (1 Gy) alone or combination and recovery period of 1, 2, 6, 12 and 24 h. (E) Representative images showing 53BP1 foci in HeLa cells treated with SCR7 (100 μM) and radiation (1 Gy) alone or in combination and recovery period of 6 h

experimental period. In contrast, the survival rate was only ~60% in the IR alone treated animals (Figure 5E).

The gross appearance of thigh, liver, and spleen from independent treatment groups showed distinct differences in the morphology of tissues following combinatorial treatment (0.5 Gy IR and SCR7), comparable to that of a normal mouse (Figure 5F). Untreated solid tumor control showed thigh tissues with infiltrated tumor cells and exhibited an increase in the size of the spleen. Although treatment with SCR7 and IR independently reduced tumor size, the effect was more prominent upon coadministration (Figure 5F). Organs like the liver exhibited no distinct morphological difference between normal, untreated, and treated animals (Figure 5F).

Histological evaluation of untreated and treated tumor mice (0.5 Gy, on 20th day of treatment) exhibited thigh muscles highly infiltrated with tumor cells. In contrast, the number of dividing cells decreased upon

SCR7 treatment (Figure 6A). Histology of the cotreated samples was similar to that of normal thigh section with intact skeletal muscles (Figure 6A). Histochemical analysis of liver section of treated mice showed no apparent structural changes than untreated tumor bearing and normal mice, further suggesting no side effects (Figure 6B). Therefore, these results demonstrate that SCR7 can potentiate radiotherapy, and coadministration can bring down the effective dose of radiation by 50%.

3.6 | Combinatorial administration of SCR7 and IR did not cause significant toxicity in mouse

Previously, different studies have reported a decrease in hematological parameters like Platelets, WBCs, Lymphocytes, Neutrophils,
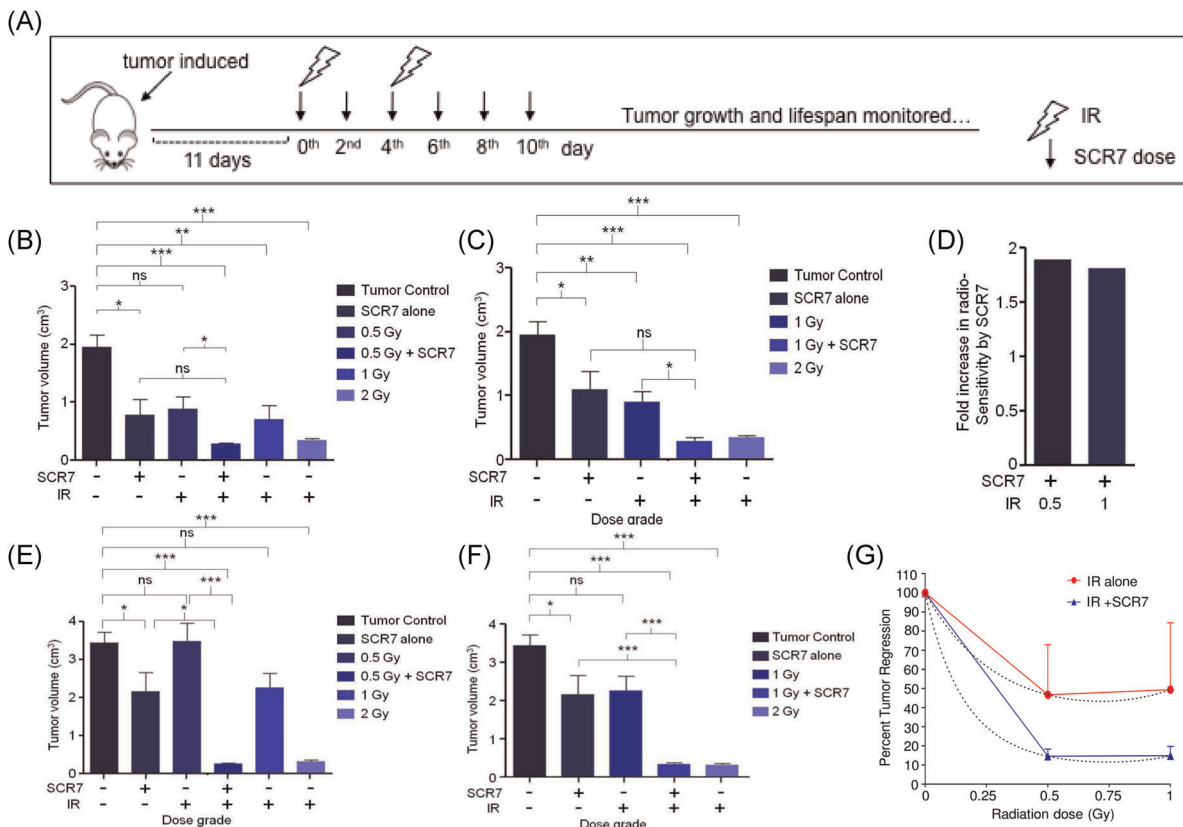
FIGURE 4 Impact of administration of SCR7 on radiation induced tumor regression in mouse Dalton's lymphoma (DLA) solid tumor model. (A) The experimental strategy used for assessing antitumor effect of SCR7 in combination with radiation in mice. Swiss albino mice were injected with DLA tumor cells, followed by administration of six doses of SCR7 (10 mg/kg), every alternate day starting from 12th day post tumor injection (0th day of tumor measurement). Mice were treated with radiation (0.5 and 1 Gy, two doses) on the 12th and 16th day of tumor development, followed by monitoring of tumor growth and/or survival for each group. (B-C) Bar graphs depicting DLA tumor progression after 16 days in mice exposed to various doses of γ-radiation either alone, or in conjunction with SCR7 (10 mg/kg). Mice were irradiated with 0.5 (B) and 1 Gy (C) of γ-rays, on 1st and 3rd day of SCR7 administration (ns: not significant, $*p < .05$, $**p < .005$, $***p < .0001$). (D) Bar graph depicting fold change in radiation sensitivity induced by SCR7 in mouse tumor models on 16th day of tumor measurement when combined with 0.5 or 1 Gy. (E-F) Bar graphs depicting DLA tumor progression after 24 days in mice exposed to γ-radiation alone or in conjunction with SCR7 (10 mg/kg). Mice were irradiated with 0.5 (E) and 1 Gy (F) of γ rays, on 1st and 3rd day of SCR7 administration (ns: not significant, $*p < .05$, $**p < .005$, $***p < .0001$). (G) Linear-quadratic model showing percent survival of mice treated with different doses of radiation and combination of SCR7 with radiation. Each point represents the mean ± SD of eight animals. The curve represents the results of the linear-quadratic fit to the data

post-irradiation and so forth.[72–76] Consistent with this, blood parameters analysis showed a noticeable reduction in WBC levels, RBC, and hemoglobin, particularly at the highest dose, when Swiss albino mice were irradiated (0.5, 1, and 2 Gy × 3 doses) (Table 1). However, when mice were exposed to IR and SCR7, the effect on WBC and RBC was marginal even at the highest dose used in the study. Further, there was no reduction in the levels of Platelets, Neutrophils, and Lymphocytes, comparable to that of vehicle control-treated animal groups or within an acceptable normal range (Table 1).

When kidney function was analyzed following the combined treatment of IR and SCR7, there was no significant difference in creatinine, blood urea nitrogen (BUN), uric acid, and phosphorous compared to normal range (Table 2). Upon serum analysis for hepatotoxicity, we found that parameters like SGPT/ALT, ALP, and bilirubin levels decreased in a dose-dependent manner following exposure to IR. However, there was no effect when mice were

treated with both SCR7 and radiation, and the levels were comparable to the accepted range (Table 3).

3.7 | Combinatorial treatment of SCR7 with IR modulates the expression of DNA damage and apoptotic proteins

Evaluation of DNA damage response was performed upon treatment of mice bearing DLA tumor with SCR7 (10 mg/kg) and radiation (0.5 and 1 Gy). Immunoblotting of tumor extracts prepared from SCR7 and IR treated samples showed an elevated expression of NHEJ protein levels KU70, KU80, and LIGASE IV were also observed in the combination cases (Figures 7A and S4). Previous reports have revealed an upregulation of KU70 upon irradiation leading to its accumulation in the nucleus.[77] This mechanism is p53 and ATM
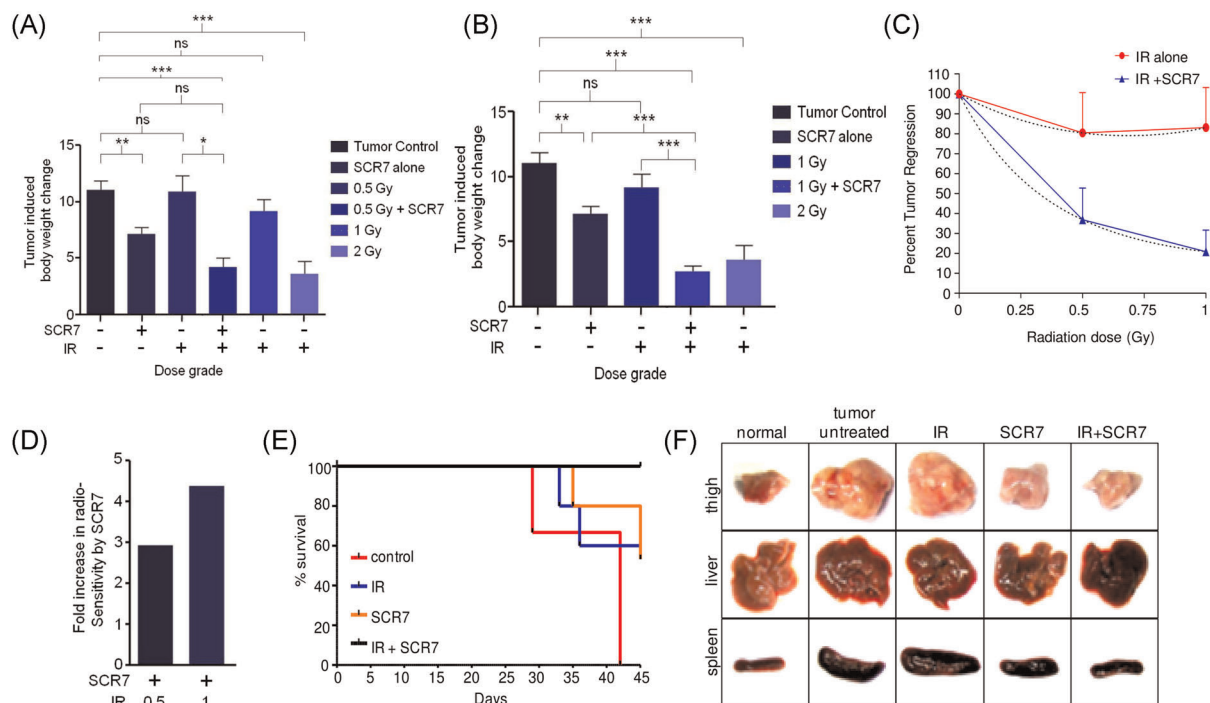
FIGURE 5 Evaluation of the impact of coadministration of SCR7 and ionizing radiation (IR) in mice bearing Dalton's lymphoma (DLA) liquid tumor. (A) Bar graph indicating tumor progression in mice after 12 days following independent treatment with SCR7 (10 mg/kg) in presence or absence of IR (0.5 Gy, 2 doses) in DLA liquid tumor model. IR was given on 1st and 3rd day of SCR7 treatment (i.e., 12th and 16th day of injection of tumor cells). "Tumor induced body weight change" indicates an increase in body weight due to overall increase in the burden of the liquid tumor, calculated by subtracting the normal weight of same aged animals from the actual weight of experimental animals to obtain the body weight increase due to tumor progression). (B) Bar graphs indicating tumor progression of DLA in mice treated with 1 Gy IR in conjunction with SCR7 (10 mg/kg) (ns: not significant, *$p < .05$, **$p < .005$, ***$p < .0001$). (C) Linear-quadratic model showing percent survival of DLA liquid tumor model treated with different doses of radiation in combination with SCR7. Each point represents the mean ± SD of eight animals. The curve represents the results of the linear-quadratic fit to the data. (D) Bar graph depicting fold change in radiation sensitivity induced by SCR7 in mouse liquid DLA tumor model on 12th day of tumor measurement when combined with 0.5 or 1 Gy (two doses) of IR. (E) Kaplan-Meier survival curve showing lifespan of mice bearing DLA tumor following co-treatment with six doses of SCR7 (10 mg/kg) and two doses of IR (0.5 Gy) or either of them alone. Untreated tumor group is indicated in red ("control"), irradiation group in blue, SCR7 treated group in orange and combination treated group in black. Survival of mice was monitored for a period of 45 days. Each experiment was repeated twice independently with 5 animals per group. (F) Gross appearance of thigh tissue/tumor, liver and spleen dissected out from normal mouse, untreated tumor-induced mouse, and those treated with radiation (0.5 Gy; two doses), SCR7 (10 mg/kg; six doses) or both

dependent. Few other studies also revealed that radiosensitivity in tumors with a high level of KU might be due to the mutation or downregulation of other DNA-damage sensing or repair proteins.[78]

Further, upon treatment with SCR7 in conjunction with 0.5 Gy IR, elevated levels of proteins involved in regulating apoptotic pathways in cancer cells, such as p-c-JUN, p-MEK1/2, p38 MAPK,[79,80] were observed compared to alone cases (Figure 7B). Elevated p-AKT level was observed upon combined treatment with 0.5 and 1 Gy IR (Figure 7B). Previous reports have revealed the phosphorylation state of p38 mitogen-activated protein kinase (P38 MAPK) upon exposure to radiation.[80–82] In cases where P38 MAPK activation was observed following exposure to IR, the P38 γ isoform was proposed to play an important role in causing radiation-induced and ATM-dependent G2/M arrest.[83]

Alterations in apoptotic protein expression were further evaluated in cotreated groups of SCR7 and IR (0.5 and 1 Gy) (Figures 7C

and S4). Levels of PARP1 and cleaved PARP1 were observed to increase in combination cases compared to control. Likewise, activated or cleaved forms of CASPASEs 3 and 9 further increased with SCR7 and radiation (both 0.5 and 1 Gy), thus suggesting activation of the intrinsic pathway of apoptosis (Figure 7C). Overall, CASPASE 3 also increased with 0.5 Gy IR, although not much improvement was observed with 1 Gy and SCR7. Elevated levels of cleaved CASPASE 8 were also seen in cotreated groups, suggesting the involvement of the extrinsic pathway. Interestingly, XRCC4 was observed to undergo phosphorylation and cleavage in the case of radiation alone, which further increased in combination with SCR7 (Figure 7C). The antiapoptotic protein BCL2 was shown to be reduced with SCR7 and 1 Gy radiation. Altogether, immunoblotting results suggest that SCR7 treatment with radiation in mice tumor models could accumulate unrepaired breaks, leading to activation of DNA damage response, and intrinsic and extrinsic pathways of apoptosis.
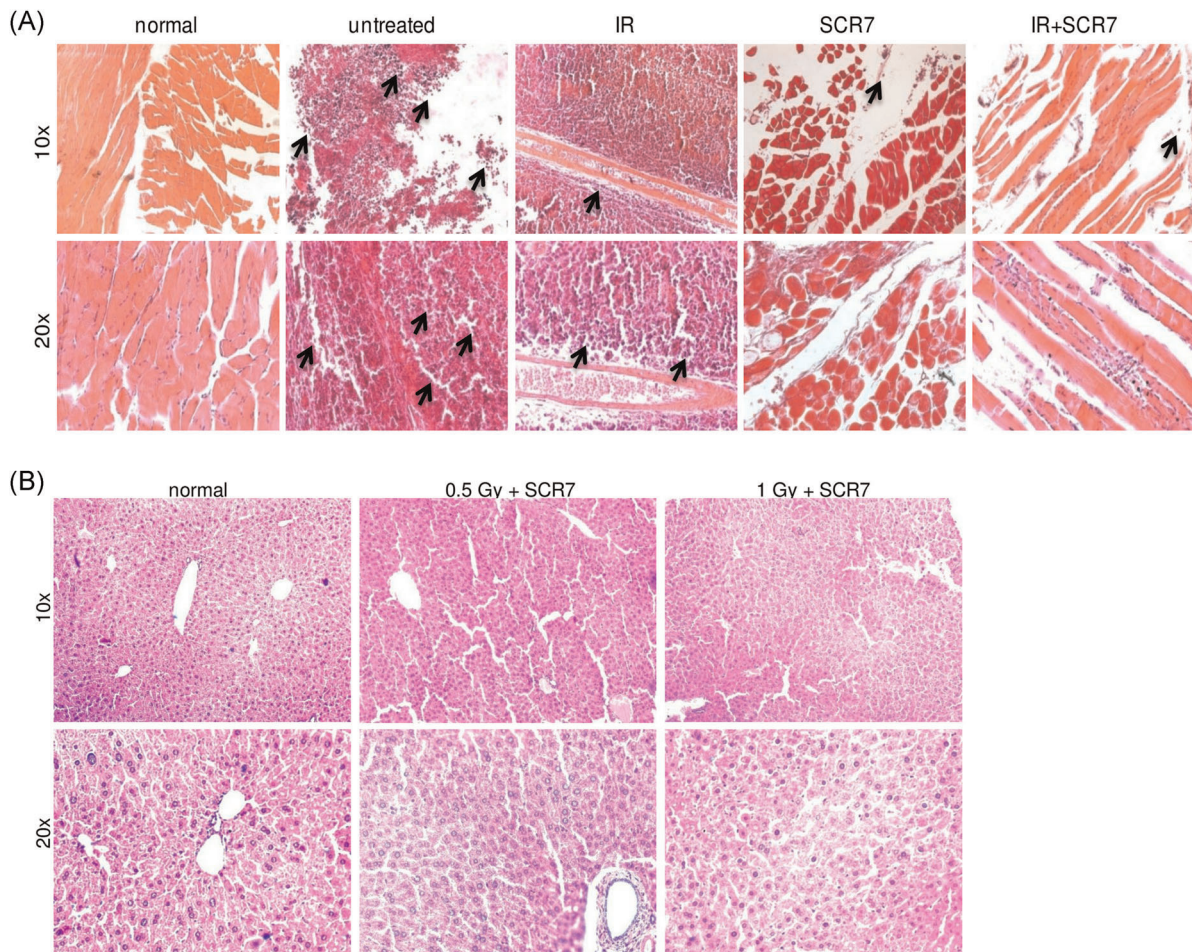
FIGURE 6 Effect of co-treatment of ionizing radiation (IR) and SCR7 in DLA mouse tumor model. (A) Representative images depicting HE staining of thigh tissue/tumor sections from mice after treatment with radiation (0.5 Gy; two doses), SCR7 (10 mg/kg; six doses) or both. All images shown represent ×10 and ×20 magnification. Arrow heads denote tumor cells. (B) Representative images showing ×10 (upper panel) and ×20 (lower panel) view of liver histology performed on 20th day of tumor development from normal group, 0.5 Gy + SCR7 and 1 Gy + SCR7 combination treatment groups, respectively

4 | DISCUSSION

SCR7, the selective and potent DNA Ligase IV/XRCC4 inhibitor identified from our laboratory, was previously reported to inhibit end resealing in NHEJ, both in vitro and in vivo.[28,40] Further, forms of SCR7, such as the autocyclized version (SCR7-cyclized) and an oxidized version (SCR7-pyrazine), also exhibited Ligase IV dependent effects, although the former was more specific inside cells.[18,41,84] Water-soluble versions, SCR7-pyrazine (Na-SCR7-P) and SCR7, and the spiro-derivative SCR130 exhibited Ligase IV dependent cytotoxicity in several cancer cell lines with accumulated double-strand breaks.[42,43,85] Apart from biochemical inhibition of NHEJ, SCR7 was used as a therapeutic agent to sensitize resistant cancers to chemotherapy and radiation; for instance, SCR7 was shown to improve the effects of radiation in DLBCL, doxorubicin in cervical cancer, and melphalan in skin cancer.[18,28,84,86] In this line, in the present study, we evaluated the antitumor efficacy of SCR7 in conjunction with different doses of radiation, thereby reducing the overall dose rate and improving survivability.

4.1 | SCR7 augments the DNA damage induced by radiation

Radiotherapy is one of the most common and well-accepted treatment modalities against cancer. Radiation kills the cancer cells by inducing single- and double-strand breaks as intermediates.[32,33,87] Evaluation of cytotoxicity of SCR7 with radiation in cancer cells revealed that SCR7 at concentrations as low as $25\,\mu M$ could lead to >50% cell death with 0.25 Gy IR. This synergistic effect in cancer cell lines was further pronounced when 50 and $100\,\mu M$ SCR7 was used together with 0.25 Gy IR. Inhibition of NHEJ inside cells by SCR7, following irradiation, led to the accumulation of unrepaired DSBs measurable by comet assay and immunofluorescence of γ-H2AX and 53BP1 inside cells. Interestingly, while the damage induced by IR was mostly repaired at early timepoints, effect of the combination of SCR7 and IR remained till 24 h, resulting in the accumulation of DSBs inside the cells. The DSBs resulted in the activation of a cascade of DNA damage response (DDR) events, which directed a coordinated

TABLE 1 Hematological analyses of mice following combinatorial administration of IR and SCR7

Hematological parameters	Control	SCR7	0.5 Gy	1 Gy	2 Gy	0.5 Gy + SCR7	1 Gy + SCR7	2 Gy + SCR7	Normal range
Platelets ($\times 10^5$/mm^3)	1.52	1.26	1.23	0.55	1.4	9.2	2.25	2.6	3–8
RBC ($\times 10^6$/mm^3)	8.82	8.6	7.47	7.57	5.7	9.25	5.93	6.5	7–13
WBC ($\times 10^3$/mm^3)	5.3	7.8	2.8	2.83	1.7	2.9	3.16	4.86	5–12
HGB (g/dl)	14.3	13.8	12	12.26	9.3	15.4	11	12.65	14–16
Neutrophils (%)	54.38	25.5	26.5	27.03	49.8	33.7	23.3	21.26	20–70
Lymphocytes (%)	40	69.4	68.2	67.1	43.8	60.5	72.6	73.2	20–70

Abbreviations: HGB, hemoglobin; RBC, red blood cells; WBC, white blood cells.

Note: Table showing analysis of blood parameters post-irradiation (0.5, 1 and 2 Gy, three doses) and after co-treatment with SCR7 (10 mg/kg).

TABLE 2 Analysis of kidney function following irradiation and co-treatment with SCR7 in mice

Renal toxicity	Control	SCR7	0.5 Gy	1 Gy	2 Gy	0.5 Gy + SCR7	1 Gy + SCR7	2 Gy +SCR7	Normal Range
Creatinine (mg/dl)	0.3	0.2	0.2	0.2	0.3	0.25	0.25	0.26	0.5–2.2
BUN (mg/dl)	15.1	8.9	11.2	9.8	10.7	13.75	10.2	9.8	10–33
Phosphorous (mg/dl)	9.05	4.3	6	3	7	5.5	5.3	3.33	5.3–8.3
Uric acid (μM)	3.83	0.16	0.2	0.3	0.4	0.25	0.43	0.26	0.1–760

Note: Analysis of kidney functions post-irradiation (0.5, 1 and 2 Gy, three doses) and after co-treatment with SCR7 (10 mg/kg).

Abbreviation: BUN, blood, urea, nitrogen.

series of signaling, thereby regulating the repair of DNA lesions.[14,88] Upon accumulation of DSBs, the MRN complex interacts with DNA ends, which recruits ATM to the DSB site, triggering ATM activation.[89] Activated ATM phosphorylates p53, a tumor suppressor protein, and H2AX, a dominant response to DSBs.[90] This phosphorylation is a prerequisite for binding MDC1 (through its BRCT domain) and the subsequent accumulation of various DDR factors at DNA lesions. Irradiation, along with SCR7 treatment, leads to enhanced DNA-PKcs mediated phosphorylation of XRCC4, implying that SCR7 indeed contributes to the DNA damaging effects exerted by irradiation. Thus, SCR7, in combination with radiation, leads to enhanced DNA damage, as shown by comet assay and an increased number of γ-H2AX foci, followed by upregulation of NHEJ proteins compared to the respective individual treatments, implying that SCR7 indeed augments radiation effects.

4.2 | SCR7 brings down the effective dose of radiation in mouse tumor models significantly by activating apoptotic pathways

Administration of SCR7 reduced the effective dose of radiation by at least 50% in both the mice solid and liquid tumor models tested. Administration of a dose of 0.5 Gy IR combined with SCR7 (10 mg/kg) showed inhibition of tumor growth with an efficiency better than that of IR dose (2 Gy) in the case of DLA tumor. Similarly, a dose of 0.5 Gy of radiation when combined with SCR7 showed an effect equivalent to 1 Gy. This enhanced effect is primarily because of inhibition of residual repair of DSBs following irradiation resulting in accumulation of breaks, as discussed above. In addition to this, we observed activation of both intrinsic and extrinsic pathways of apoptosis in DLA solid tumors treated with SCR7 alongside radiation. We also observed phosphorylation and cleavage of XRCC4 in co-treatment groups. The combination treatment further led to the downregulation of BCL2, an antiapoptotic protein essential for activating the apoptotic pathway.[40] Observed activation of Caspases resulted in cleavage of PARP1 followed by DNA fragmentation and eventually cell death, which is consistent with previous studies.[40,91] In one of our previous reports [40] we have further showed by TUNEL assay on tumor tissues that DNA fragmentation as a result of apoptotic signaling cascades resulted in a significant elimination of tumor cells following combination treatments. Thus, the combination of SCR7 and radiation can sensitize cancer cells by augmenting the DNA damaging effects exerted by γ-radiation through effective blocking of NHEJ and by inducing multiple pathways of apoptosis.

4.3 | SCR7 can improve the efficacy of radiation by reducing the side effects

Although radiotherapy is used effectively for treating many cancers, including breast cancer and lymphoma, it often causes side effects, like other cancer therapeutic regimes. Side effects differ for

TABLE 3 Analysis of liver function following irradiation and co-treatment with SCR7 in mice

Hepatotoxicity	Control	SCR7	0.5 Gy	1 Gy	2 Gy	0.5 Gy + SCR7	1 Gy + SCR7	2 Gy + SCR7	Normal range
SGPT/ALT (U/L)	48.65	57.73	40	33.1	25.1	65	58.7	51.5	10–35
Albumin (g/dl)	3.06	2.03	3.3	3.05	3	3.3	2.3	3.5	3.8–4.8
Bilirubin (mg/dl)	0.58	0.86	0.3	0.35	0.4	0.6	0.6	0.43	0.2–0.55
ALP (U/L)	255.9	313.7	320	251.5	115.2	272.6	295	155.6	62–230
Total protein (g/dl)	6.05	3.66	3.3	4.6	6.8	5.4	3.8	3.6	4.5–6.5

Note: Analysis of hepatotoxicity post-irradiation (0.5, 1 and 2 Gy, three doses) and after co-treatment with SCR7 (10 mg/kg).

Abbreviations: ALP, alkaline phosphatase; ALT denotes alanine aminotransferase; SGPT, serum glutamic pyruvic transaminase.
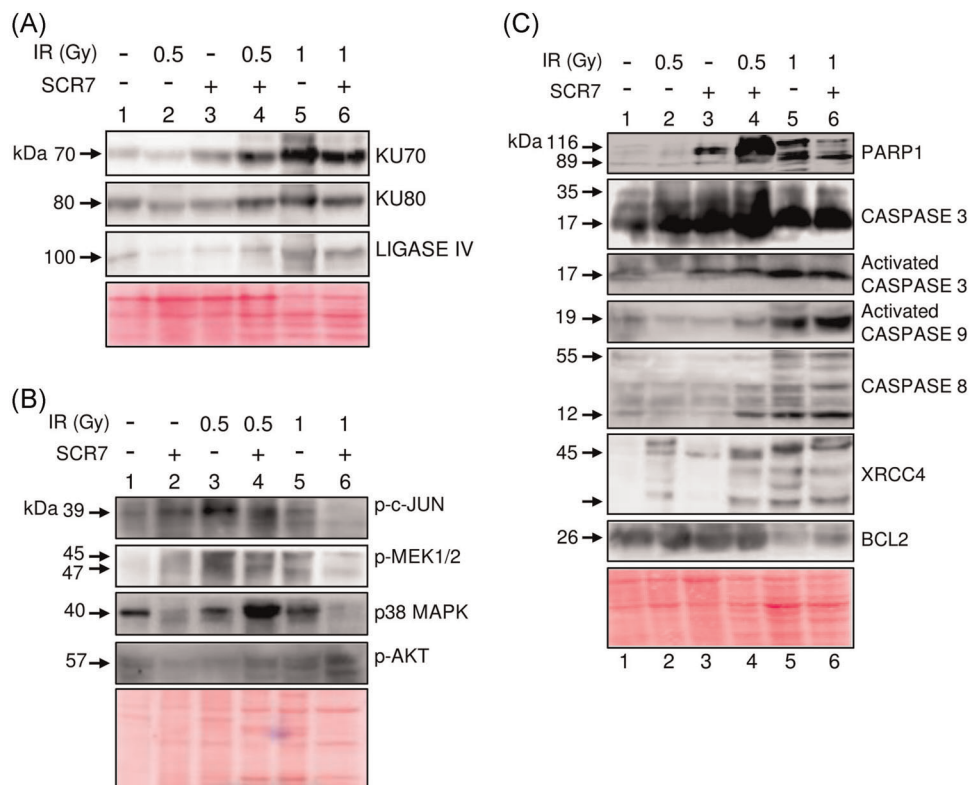
FIGURE 7 Mechanism of antitumor effects induced upon combinatorial treatment of ionizing radiation (IR) and SCR7. (A) Western blot analysis of DNA repair proteins (KU70, KU80, and Ligase IV) in Dalton's lymphoma (DLA) tumor-induced mice upon treatment with six doses of SCR7 (10 mg/kg) and two doses each of IR (0.5 and 1 Gy). Each experiment was repeated a minimum of two independent times and the representative blot has been shown. Ponceau stained membrane served as the loading control. (B) Western blot analysis for MAP Kinase pathway proteins that are activated by ROS generated from ionizing radiation. (C) Western blot images showing the mechanism of apoptosis upon coadministration of SCR7 and IR in tumor-bearing mice as assessed on 20th day of tumor measurement. Ponceau stained membrane served as the loading control in all the cases

individuals based on the type of cancer and general health of a person, including the immune system's effectiveness. Consistent with this, we have also seen variability in sensitivity towards both radiation and SCR7 in animal models. Although newer technologies are used for irradiation with precision, the higher doses used during therapy can damage normal cells, in addition to the actual target i.e., the cancer cells. Generally, multiples of 2 Gy of radiation per day are given in multiple sessions to patients.[24,92] Combining a therapeutic agent targeting an important DNA repair pathway in cancer with gold standard treatment modalities such as radiation could improve the efficacy.

Using various mice tumor models, our study revealed that SCR7 could bring down the radiation dose by at least 50%. We also observed that mice receiving a co-treatment of SCR7 and radiation did not develop any side effects, as observed from blood parameters, kidney-function tests, and histological analysis of tissues, which is indeed remarkable since it might help in significantly reducing the side effects of radiotherapy if extended to cancer patients. Although further studies are required before these findings could be extended to clinics, it is indeed a promising lead and needs to be explored further.

ORCID

Bibha Choudhary http://orcid.org/0000-0001-7173-0682
Sathees C. Raghavan http://orcid.org/0000-0003-3003-1417

REFERENCES

1. Davis AJ, Chen DJ. DNA double strand break repair via non-homologous end-joining. *Translat Cancer Res*. 2013;2(3):130-143.

2. Nishana M, Raghavan SC. Role of recombination activating genes in the generation of antigen receptor diversity and beyond. *Immunology*. 2012;137(4):271-281.

3. Friedberg EC, Aguilera A, Gellert M, et al. DNA repair: from molecular mechanism to human disease. *DNA Repair*. 2006;5(8):986-996.

4. Kryston TB, Georgiev AB, Pissis P, Georgakilas AG. Role of oxidative stress and DNA damage in human carcinogenesis. *Mutat Res*. 2011;711(1-2):193-201.

5. Nambiar M, Raghavan SC. How does DNA break during chromosomal translocations? *Nucleic Acids Res*. 2011;39(14):5813-5825.

6. Ray U, Raghavan SC. Modulation of DNA double-strand break repair as a strategy to improve precise genome editing. *Oncogene*. 2020;39(41):6393-6405.

7. Zhu C, Mills KD, Ferguson DO, et al. Unrepaired DNA breaks in p53-deficient cells lead to oncogenic gene amplification subsequent to translocations. *Cell*. 2002;109(7):811-821.

8. Nambiar M, Kari V, Raghavan SC. Chromosomal translocations in cancer. *Biochim Biophys Acta*. 2008;1786(2):139-152.

9. Iliakis G, Wang H, Perrault AR, et al. Mechanisms of DNA double strand break repair and chromosome aberration formation. *Cytogenet Genome Res*. 2004;104(1-4):14-20.

10. Nambiar M, Raghavan SC. Chromosomal translocations among the healthy human population: implications in oncogenesis. *Cell Mol Life Sci*. 2013;70(8):1381-1392.

11. Raghavan SC, Lieber MR. Chromosomal translocations and non-B DNA structures in the human genome. *Cell Cycle*. 2004;3(6):762-768.

12. Iliakis G. Backup pathways of NHEJ in cells of higher eukaryotes: cell cycle dependence, radiotherapy and oncology. *J Eur Soc Ther Radiol Oncol*. 2009;92(3):310-315.

13. Srivastava M, Raghavan SC. DNA double-strand break repair inhibitors as cancer therapeutics. *Chem Biol*. 2015;22(1):17-29.

14. Wyman C, Kanaar R. DNA double-strand break repair: all's well that ends well. *Annu Rev Genet*. 2006;40:363-383.

15. Lieber MR. The mechanism of double-strand DNA break repair by the nonhomologous DNA end-joining pathway. *Annu Rev Biochem*. 2010;79:181-211.

16. Sharma S, Javadekar SM, Pandey M, Srivastava M, Kumari R, Raghavan SC. Homology and enzymatic requirements of microhomology-dependent alternative end joining. *Cell Death Dis*. 2015;6:e1697.

17. Deriano L, Roth DB. Modernizing the nonhomologous end-joining repertoire: alternative and classical NHEJ share the stage. *Annu Rev Genet*. 2013;47:433-455.

18. Ray U, Raghavan SC. Inhibitors of DNA double-strand break repair at the crossroads of cancer therapy and genome editing. *Biochem Pharmacol*. 2020;182:114195.

19. Ochi T, Blackford AN, Coates J, et al. DNA repair. PAXX, a paralog of XRCC4 and XLF, interacts with Ku to promote DNA double-strand break repair. *Science*. 2015;347(6218):185-188.

20. Kumari N, Raghavan SC. G-quadruplex DNA structures and their relevance in radioprotection. *Biochim Biophys Acta*. 2021;1865(5):129857.

21. Ghosh D, Raghavan SC. Nonhomologous End Joining: new accessory factors fine tune the machinery. *Trends Genet*. 2021;37:582-599.

22. Ghosh D, Raghavan SC. 20 years of DNA polymerase m, the polymerase that still surprises [published online ahead of print March 31, 2021]. *FEBS J*. 2021. https://doi.org/10.1111/febs.15852

23. Clarke M, Collins R, Darby S, et al, Early Breast Cancer Trialists' Collaborative. Effects of radiotherapy and of differences in the extent of surgery for early breast cancer on local recurrence and 15-year survival: an overview of the randomisedtrials. *Lancet*. 2005;366(9503):2087-2106.

24. Begg AC, Stewart FA, Vens C. Strategies to improve radiotherapy with targeted drugs. *Nat Rev Cancer*. 2011;11(4):239-253.

25. Witkowska M, Majchrzak A, Smolewski P. The role of radiotherapy in Hodgkin's lymphoma: what has been achieved during the last 50 years? *BioMed Res Int*. 2015;2015:485071.

26. Zimmermann M, Oehler C, Mey U, Ghadjar P, Zwahlen DR. Radiotherapy for Non-Hodgkin's lymphoma: still standard practice and not an outdated treatment option. *Rad Oncol*. 2016;11(1):110.

27. Press OW, Li H, Schoder H, et al. US Intergroup Trial of response-adapted therapy for stage III to IV Hodgkin lymphoma using early interim fluorodeoxyglucose-positron emission tomography imaging: Southwest Oncology Group S0816. *J Clin Oncol*. 2016;34(17):2020-2027.

28. Gopalakrishnan V, Radha G, Raghavan SC, Choudhary B. Inhibitor of nonhomologous end joining can inhibit proliferation of diffuse large B-Cell lymphoma cells and potentiate the effect of ionization radiation. *J Rad Cancer Res*. 2018;9(2):93-101.

29. Bentzen SM. Preventing or reducing late side effects of radiation therapy: radiobiology meets molecular pathology. *Nat Rev Cancer*. 2006;6(9):702-713.

30. Cannan WJ, Pederson DS. Mechanisms and consequences of double-strand DNA break formation in chromatin. *J Cell Physiol*. 2016;231(1):3-14.

31. Lewanski CR, Gullick WJ. Radiotherapy and cellular signalling. *Lancet Oncol*. 2001;2(6):366-370.

32. O'Connor MJ. Targeting the DNA damage response in cancer. *Mol Cell*. 2015;60(4):547-560.

33. Vignard J, Mirey G, Salles B. Ionizing-radiation induced DNA double-strand breaks: a direct and indirect lighting up. *Radiother Oncol*. 2013;108(3):362-369.

34. Gopalakrishnan V, Dahal S, Radha G, Sharma S, Raghavan SC, Choudhary B. Characterization of DNA double-strand break repair pathways in diffuse large B cell lymphoma. *Mol Carcinog*. 2019;58(2):219-233.

35. Pucci S, Mazzarelli P, Rabitti C, et al. Tumor specific modulation of KU70/80 DNA binding activity in breast and bladder human tumor biopsies. *Oncogene*. 2001;20(6):739-747.

36. Shintani S, Mihara M, Li C, et al. Up-regulation of DNA-dependent protein kinase correlates with radiation resistance in oral squamous cell carcinoma. *Cancer Sci*. 2003;94(10):894-900.

37. Sirzen F, Nilsson A, Zhivotovsky B, Lewensohn R. DNA-dependent protein kinase content and activity in lung carcinoma cell lines: correlation with intrinsic radiosensitivity. *Eur J Cancer*. 1999;35(1):111-116.

38. Han J, Hankinson SE, Ranu H, De Vivo I, Hunter DJ. Polymorphisms in DNA double-strand break repair genes and breast cancer risk in the Nurses' Health Study. *Carcinogenesis*. 2004;25(2):189-195.

39. Riballo E, Doherty AJ, Dai Y, et al. Cellular and biochemical impact of a mutation in DNA ligase IV conferring clinical radiosensitivity. *J Biol Chem*. 2001;276(33):31124-31132.

40. Srivastava M, Nambiar M, Sharma S, et al. An inhibitor of nonhomologous end-joining abrogates double-strand break repair and impedes cancer progression. *Cell*. 2012;151:1474-1487.

41. Vartak SV, Swarup HA, Gopalakrishnan V, et al. Autocyclized and oxidized forms of SCR7 induce cancer cell death by inhibiting nonhomologous DNA end joining in a Ligase IV dependent manner. *FEBS J*. 2018;285(21):3959-3976.

42. Pandey M, Gopalakrishnan V, Swarup H, et al. Water-soluble version of SCR7-pyrazine inhibits DNA repair and abrogates tumor cell proliferation. *J Rad Cancer Res*. 2019;10(1):27-43.

43. Ray U, Jose A, Suresh R, et al. Water-soluble SCR7 can abrogate DNA end joining and induce cancer cell death. *Clin Oncol Res*. 2020:1-7.

44. Ray U, Vartak SV, Raghavan SC. NHEJ inhibitor SCR7 and its different forms: promising CRISPR tools for genome engineering. *Gene*. 2020;763:144997.

45. Manjunath M, Choudhary B, Raghavan SC. SCR7, a potent cancer therapeutic agent and a biochemical inhibitor of nonhomologous DNA end-joining. *Cancer Reports*. 2021:e1341.

46. Kumari N, Vartak SV, Dahal S, et al. G-quadruplex structures contribute to differential radiosensitivity of the human genome [published online ahead of print March 31, 2021]. *iScience*. 2019;21: 288-307.

47. Kumar TS, Kari V, Choudhary B, Nambiar M, Akila TS, Raghavan SC. Anti-apoptotic protein BCL2 down-regulates DNA end joining in cancer cells. *J Biol Chem*. 2010;285(42):32657-32670.

48. Kavitha CV, Nambiar M, Narayanaswamy PB, et al. Propyl-2-(8-(3,4-difluorobenzyl)-2',5'-dioxo-8-azaspiro[bicyclo[3.2.1] octane-3,4'-imidazolidine]-1'-yl) acetate induces apoptosis in human leukemia cells through mitochondrial pathway following cell cycle arrest. *PLOS One*. 2013;8(7):e69103.

49. Sharath Kumar KS, Hanumappa A, Vetrivel M, et al. Anti-proliferative and tumor inhibitory studies of 2,3 disubstituted 4-thiazolidinone derivatives. *Bioorg Med Chem Lett*. 2015;25(17): 3616-3620.

50. Thomas E, Gopalakrishnan V, Hegde M, et al. A novel resveratrol based tubulin inhibitor induces mitotic arrest and activates apoptosis in cancer cells. *Sci Rep*. 2016;6:34653.

51. Hegde M, Mantelingu K, Pandey M, Pavankumar CS, Rangappa KS, Raghavan SC. Combinatorial study of a novel poly (ADP-ribose) polymerase inhibitor and an HDAC inhibitor, SAHA, in leukemic cell lines. *Target Oncol*. 2016;11(5):655-665.

52. Iyer D, Vartak SV, Mishra A, et al. Identification of a novel BCL2-specific inhibitor that binds predominantly to the BH1 domain. *FEBS J*. 2016;283(18):3408-3437.

53. Vartak SV, Hegde M, Iyer D, et al. A novel inhibitor of BCL2, Disarib abrogates tumor growth while sparing platelets, by activating intrinsic pathway of apoptosis. *Biochem Pharmacol*. 2016;122:10-22.

54. Sebastian R, Raghavan SC. Induction of DNA damage and erroneous repair can explain genomic instability caused by endosulfan. *Carcinogenesis*. 2016;37(10):929-940.

55. Hegde M, Vartak SV, Kavitha CV, et al. A benzothiazole derivative (5g) induces DNA damage and potent G2/M arrest in cancer cells. *Sci Rep*. 2017;7(1):2533.

56. John F, George J, Vartak SV, et al. Enhanced efficacy of pluronic copolymer micelle encapsulated SCR7 against cancer cell proliferation. *Macromol Biosci*. 2015;15(4):521-534.

57. Shahabuddin MS, Nambiar M, Moorthy BT, et al. A novel structural derivative of natural alkaloid ellipticine, MDPSQ, induces necrosis in leukemic cells. *Invest New Drugs*. 2011;29(4):523-533.

58. Sharma S, Panjamurthy K, Choudhary B, et al. A novel DNA intercalator, 8-methoxy pyrimido[4',5':4,5]thieno (2,3-b)quinoline-4(3H)-one induces apoptosis in cancer cells, inhibits the tumor progression and enhances lifespan in mice with tumor. *Mol Carcinog*. 2013;52(6):413-425.

59. Srivastava M, Hegde M, Chiruvella KK, et al. Sapodilla plum (Achras sapota) induces apoptosis in cancer cell lines and inhibits tumor progression in mice. *Sci Rep*. 2014;4:6147.

60. Thomas E, Gopalakrishnan V, Somasagara RR, Choudhary B, Raghavan SC. Extract of vernonia condensata, inhibits tumor progression and improves survival of tumor-allograft bearing mouse. *Sci Rep*. 2016;6:23255.

61. Somasagara RR, Hegde M, Chiruvella KK, Musini A, Choudhary B, Raghavan SC. Extracts of strawberry fruits induce intrinsic pathway of apoptosis in breast cancer cells and inhibits tumor progression in mice. *PLOS One*. 2012;7(10):e47021.

62. Srivastava S, Somasagara RR, Hegde M, et al. Quercetin, a natural flavonoid interacts with DNA, arrests cell cycle and causes tumor regression by activating mitochondrial pathway of apoptosis. *Sci Rep*. 2016;6:24049.

63. Sebastian R, Raghavan SC. Endosulfan induces male infertility. *Cell Death Dis*. 2015;6(12):e2022.

64. Chiruvella KK, Panjamurthy K, Choudhary B, Joy O, Raghavan SC. Methyl angolensate from callus of Indian redwood induces cytotoxicity in human breast cancer cells. *Int J Biomed Sci*. 2010;6(3): 182-194.

65. Sharma S, Choudhary B, Raghavan SC. Efficiency of nonhomologous DNA end joining varies among somatic tissues, despite similarity in mechanism. *Cell Mol Life Sci*. 2011;68(4):661-676.

66. Dahal S, Dubey S, Raghavan SC. Homologous recombination-mediated repair of DNA double-strand breaks operates in mammalian mitochondria. *Cell Mol Life Sci*. 2018;75(9):1641-1655.

67. Bodgi L, Canet A, Pujo-Menjoue Lt, Lesne A, Victor JM, Foray N. Mathematical models of radiation action on living cells: from the target theory to the modern approaches. A historical and critical review. *J Theor Biol*. 2016;394:93-101.

68. Brenner DJ. The linear-quadratic model is an appropriate methodology for determining isoeffective doses at large doses per fraction. *Semin Radiat Oncol*. 2008;18(4):234-239.

69. Chadwick KH, Leenhouts HP. A molecular theory of cell survival. *Phys Med Biol*. 1973;18(1):78-87.

70. Chou TC, Martin N. The mass-action law-based new computer software, CompuSyn, for automated simulation of synergism and antagonism in drug combination studies. *Cancer Res*. 2007;67(9 Suppl):637.

71. Sharma S, Varsha KK, Kumari S, et al. Acute toxicity analysis of Disarib, an inhibitor of BCL2. *Sci Rep*. 2020;10(1):15188.

72. Shanshoury HEI, Shanshoury GEI, Abaza A. Evaluation of low dose ionizing radiation effect on some blood components in animal model. *J Radiat Res Appl Si*. 2016;9(3):282-293.

73. Ware JH, Sanzari J, Avery S, et al. Effects of proton radiation dose, dose rate and dose fractionation on hematopoietic cells in mice. *Radiat Res*. 2010;174(3):325-330.

74. Sanzari JK, Wan XS, Krigsfeld GS, Wroe AJ, Gridley DS, Kennedy AR. The effects of gamma and proton radiation exposure on hematopoietic cell counts in the Ferret model. *Gravitat Space Res*. 2013;1(1):79-94.

75. Gridley DS, Pecaut MJ, Miller GM, Moyers MF, Nelson GA. Dose and dose rate effects of whole-body gamma-irradiation: II. Hematological variables and cytokines. *In Vivo*. 2001;15(3):209-216.

76. Maks CJ, Wan XS, Ware JH, et al. Analysis of white blood cell counts in mice after gamma- or proton-radiation exposure. *Radiat Res*. 2011;176(2):170-176.

77. Brown KD, Lataxes TA, Shangary S, et al. Ionizing radiation exposure results in up-regulation of Ku70 via a p53/ataxia-telangiectasia-mutated protein-dependent mechanism. *J Biol Chem*. 2000;275(9):6651-6656.

78. Wilson CR, Davidson SE, Margison GP, Jackson SP, Hendry JH, West CM. Expression of Ku70 correlates with survival in carcinoma of the cervix. *Br J Cancer*. 2000;83(12):1702-1706.

79. Deng Z, Sui G, Rosa PM, Zhao W. Radiation-induced c-Jun activation depends on MEK1-ERK1/2 signaling pathway in microglial cells. *PLOS One*. 2012;7(5):e36739.

80. Dent P, Yacoub A, Fisher PB, Hagan MP, Grant S. MAPK pathways in radiation responses. *Oncogene*. 2003;22(37):5885-5896.

81. Tessner TG, Muhale F, Schloemann S, Cohn SM, Morrison AR, Stenson WF. Ionizing radiation up-regulates cyclooxygenase-2 in I407 cells through p38 mitogen-activated protein kinase. *Carcinogenesis*. 2004;25(1):37-45.

82. Wang Y, Liu L, Zhou D. Inhibition of p38 MAPK attenuates ionizing radiation-induced hematopoietic cell senescence and residual bone marrow injury. *Radiat Res*. 2011;176(6):743-752.

83. Wang X, McGowan CH, Zhao M, et al. Involvement of the MKK6-p38gamma cascade in gamma radiation-induced cell cycle arrest. *Mol Cell Biol*. 2000;20(13):4543-4552.

84. Manjunath M, Choudhary B, Raghavan SC. SCR7, a potent cancer therapeutic agent and a biochemical inhibitor of nonhomologous DNA end-joining. *Cancer Reports*. 2021:e1341.

85. Ray U, Raul SK, Gopinatha VK, et al. Identification and characterization of novel SCR7-based small-molecule inhibitor of DNA

end-joining, SCR130 and its relevance in cancer therapeutics. *Mol Carcinog*. 2020;59(6):618-628.

86. Vartak SV, Raghavan SC. Inhibition of nonhomologous end joining to increase the specificity of CRISPR/Cas9 genome editing. *FebsJ*. 2015;282(22):4289-4294.

87. Mehta A, Haber JE. Sources of DNA double-strand breaks and models of recombinational DNA repair. *Cold Spring Harbor Perspect Biol*. 2014;6(9):a016428.

88. Huen MS, Chen J. Assembly of checkpoint and repair machineries at DNA damage sites. *Trends Biochem Sci*. 2010;35(2):101-108.

89. Lee JH, Paull TT. ATM activation by DNA double-strand breaks through the Mre11-Rad50-Nbs1 complex. *Science*. 2005;308(5721):551-554.

90. Sedelnikova OA, Bonner WM. GammaH2AX in cancer cells: a potential biomarker for cancer diagnostics, prediction and recurrence. *Cell Cycle*. 2006;5(24):2909-2913.

91. D'Amours D, Sallmann FR, Dixit VM, Poirier GG. Gain-of-function of poly(ADP-ribose) polymerase-1 upon cleavage by apoptotic proteases: implications for apoptosis. *J Cell Sci*. 2001;114(Pt 20):3771-3778.

92. Wang L, Correa CR, Zhao L, et al. The effect of radiation dose and chemotherapy on overall survival in 237 patients with Stage III non-small-cell lung cancer. *Int J Radiat Oncol Biol Phys*. 2009;73(5):1383-1390.

SUPPORTING INFORMATION

Additional Supporting Information may be found online in the supporting information tab for this article.